An Investigation of G-Quadruplex Structural Polymorphism in the Human Telomere Using a Combined Approach of Hydrodynamic Bead Modeling and Molecular Dynamics Simulation

Huy T. Le[1], William L. Dean[1,2], Robert Buscaglia[1], Jonathan B. Chaires[1,2,3], and John O. Trent[1,2,3]*

[1]Department of Biochemistry and Molecular Biology, School of Medicine, University of Louisville, HSC-A Building, Room 616, Louisville, KY 40202,

[2]James Graham Brown Cancer Center, University of Louisville, 529 South Jackson Street, Louisville, KY 40202,

[3]Department of Medicine, School of Medicine, University of Louisville, 550 South Jackson Street, Louisville, KY 40202

Supporting Information

Table of Content

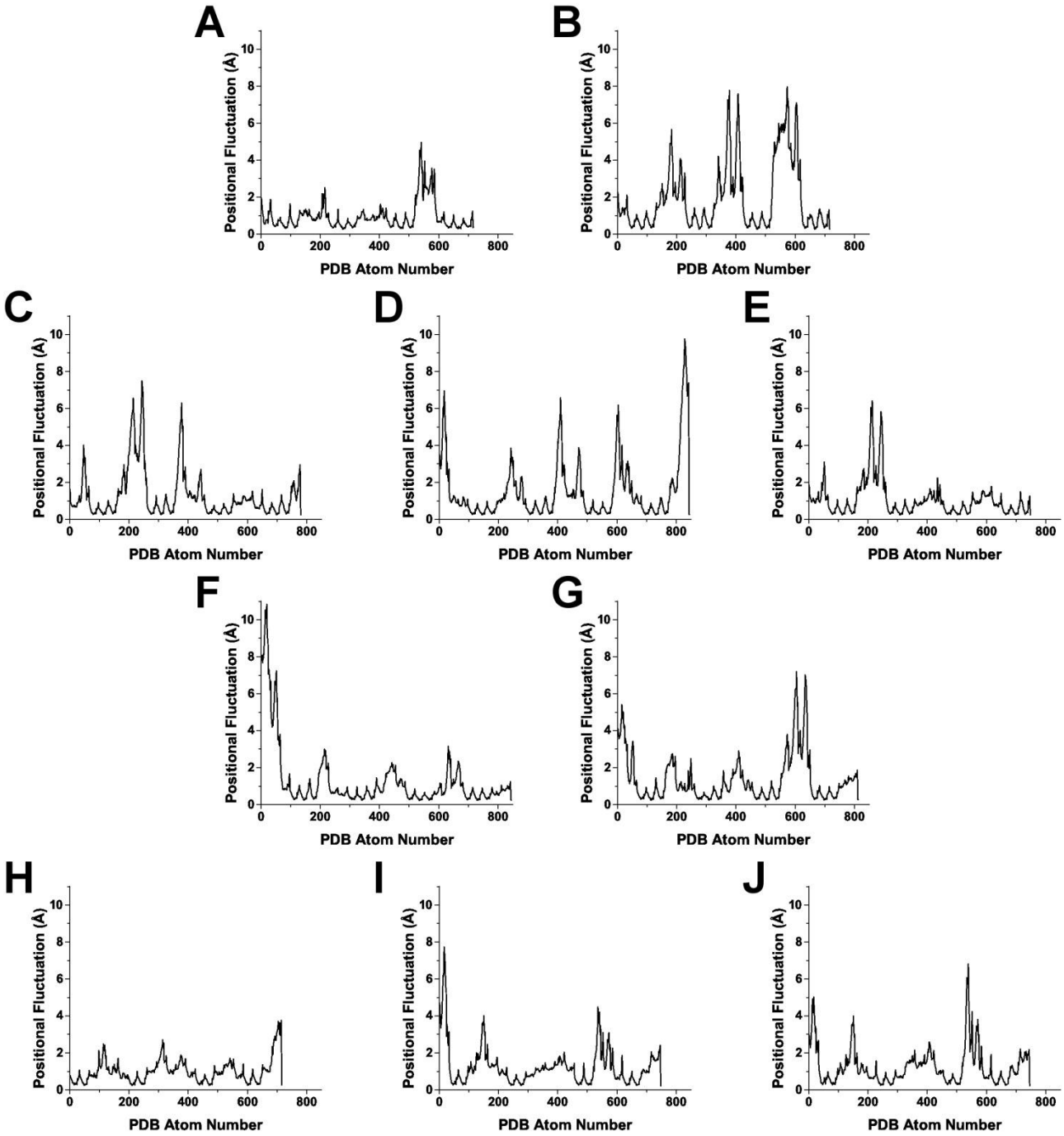

Figure S1. Per-atom atomic positional fluctuations over 10,000 frames for 143D (A), 1KF1 (B), 2GKU (C), 2HY9 (D), 2JSM (E), 2JPZ (F), 2JSL (G), 2KF8 (H), 2KKA-G (I), and 2KKA-I (J).

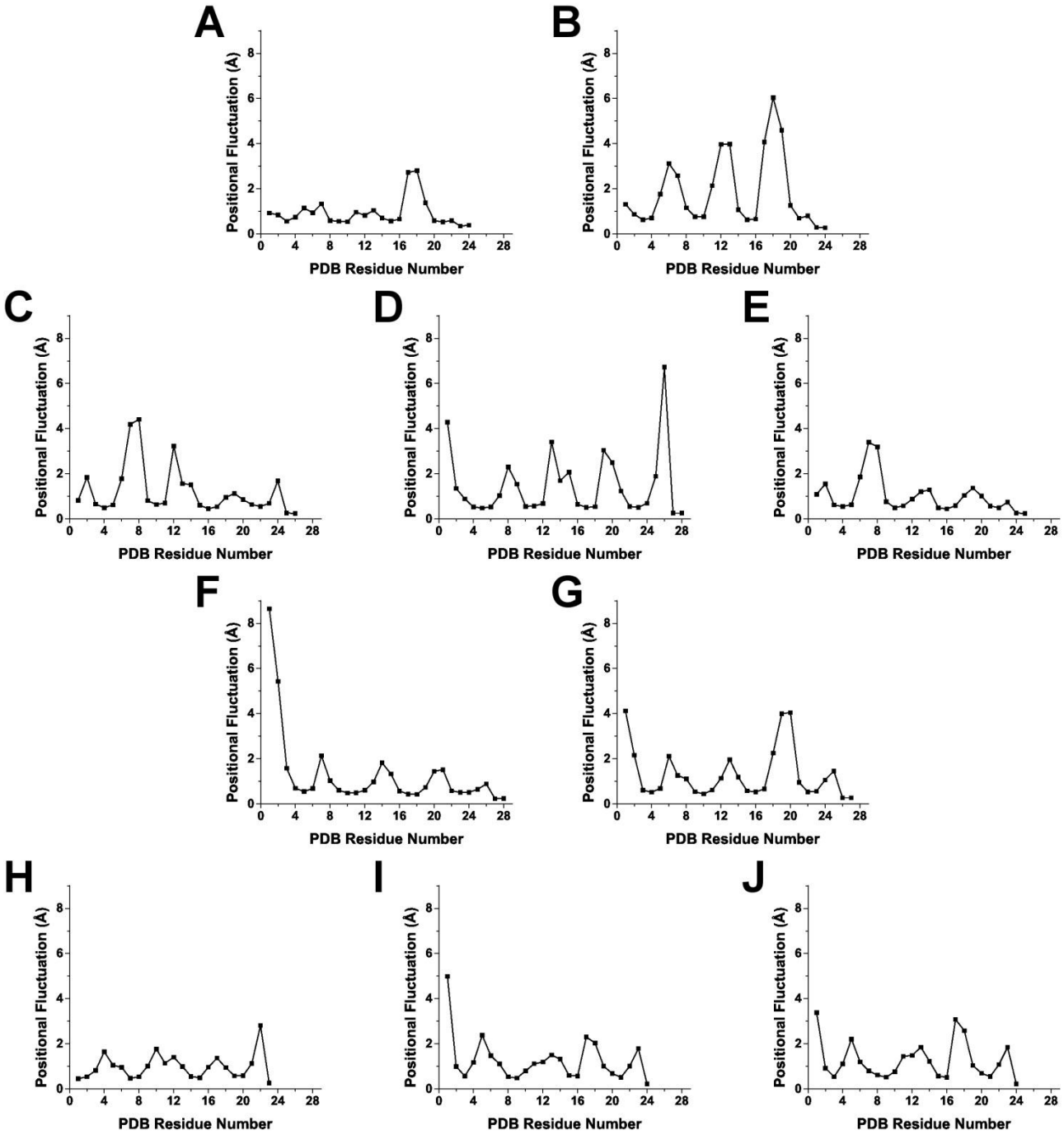

Figure S2. Per-residue atomic positional fluctuations over 10,000 frames for 143D (A), 1KF1 (B), 2GKU (C), 2HY9 (D), 2JSM (E), 2JPZ (F), 2JSL (G), 2KF8 (H), 2KKA-G (I), and 2KKA-I (J).

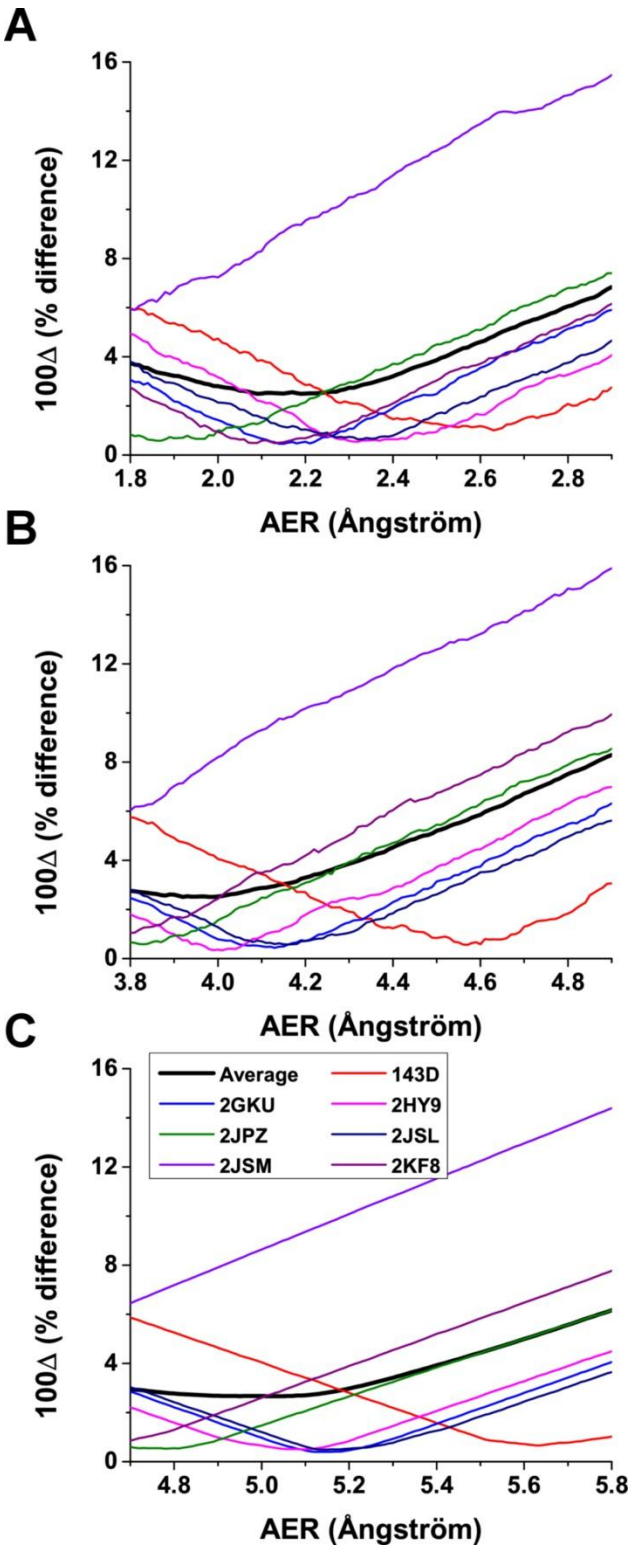

Figure S3. HYDROPRO parameters calibrated by global fitting of translational equivalent radii with AUC data. Translational equivalent radius is also known as the Stokes radius. The values for 100ΔX and 100Δ as a function of the atomic element radius (AER) for the primary hydrodynamic model as calculated using the seven G-quadruplex structures formed from the human telomere sequence. Hydrodynamic properties of G-quadruplexes were calculated using the atomic-level hydrodynamic shell-model calculation (A), residue-level shell-model calculation (B), and residue-level bead-model calculation (C).

Table S1. Comparisons of $s_{20,W}$ Calculated from MD Simulations and NMR Structures

Structure	% Diff. Atom/shell	%Diff. Residue/shell	%Diff. Residue/bead
143D	3.05 %	0.06 %	0.34 %
2GKU	0.32 %	1.87 %	2.03 %
2HY9	5.30 %	3.04 %	3.38 %
2JPZ	1.17 %	0.31 %	0.28 %
2JSL	0.09 %	0.98 %	0.71 %
2JSM	1.35 %	3.61 %	3.11 %
2KF8	2.44 %	2.64 %	2.69 %
Weighted Average[1]	1.85 %	1.89 %	1.88 %

[1]Average weighted by number of poses deposited in PDB Database (143D – 6 poses, 2GKU – 12 poses, 2HY9 – 10 poses, 2JPZ – 10 poses, 2JSL – 10 poses, 2JSM – 10 poses, 2KF8 – 10 poses)

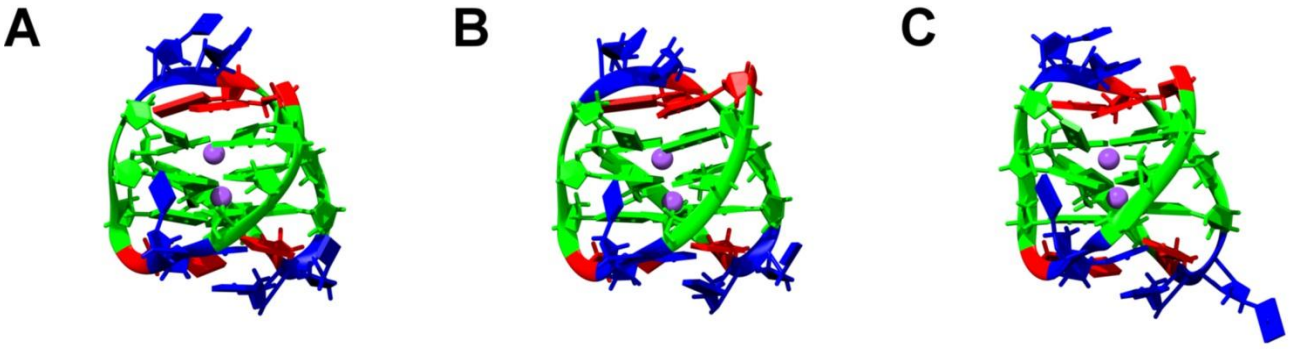

Figure S4. Cartoon depictions of representative structures from cluster analysis of the 143D MD trajectory. The clusters are shown from the most populated cluster to the least populated cluster. Nucleotides are colored according to NDB formats: guanine is green, adenine is red, and thymine is blue. Sodium ions are colored purple.

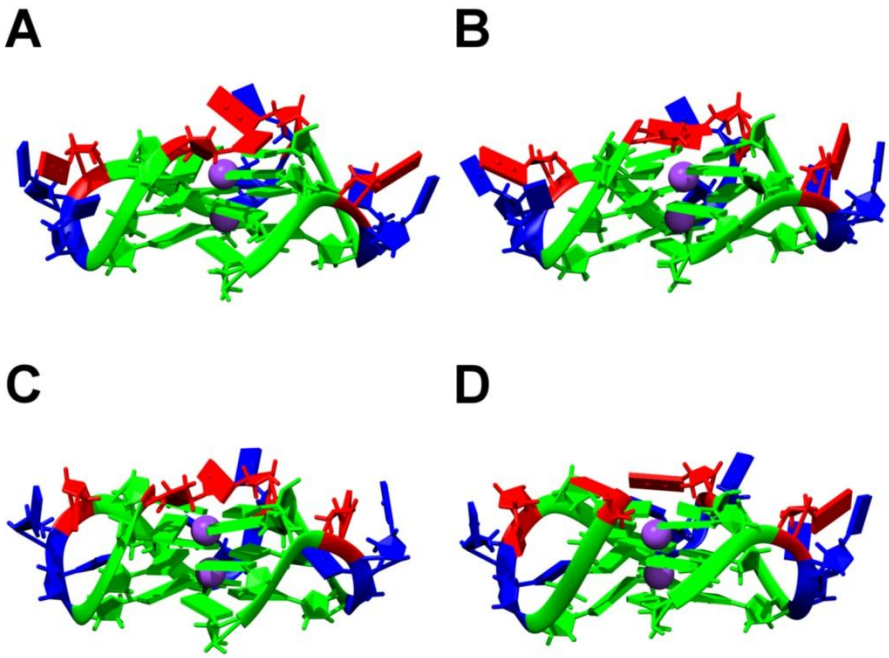

Figure S5. Cartoon depictions of representative structures from cluster analysis of the 1KF1 MD trajectory. The clusters are shown from the most populated cluster to the least populated cluster. Nucleotides are colored according to NDB formats: guanine is green, adenine is red, and thymine is blue. Potassium ions are colored purple.

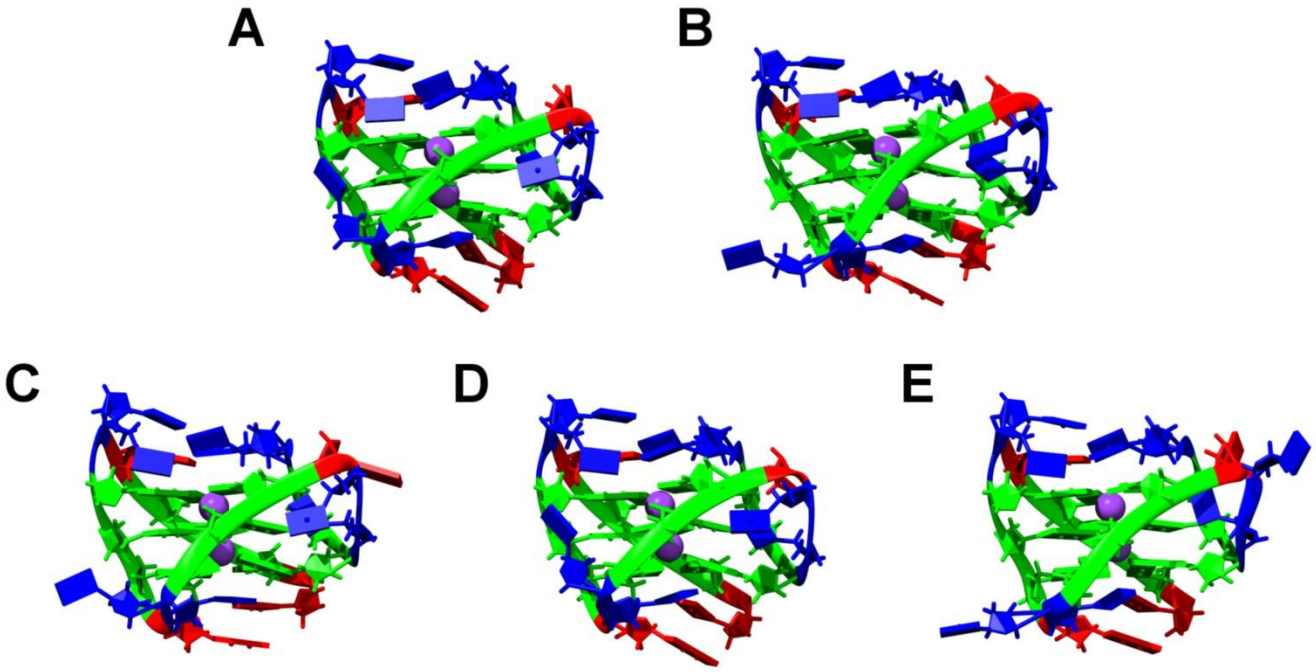

Figure S6. Cartoon depictions of representative structures from cluster analysis of the 2GKU MD trajectory. The clusters are shown from the most populated cluster to the least populated cluster. Nucleotides are colored according to NDB formats: guanine is green, adenine is red, and thymine is blue. Potassium ions are colored purple.

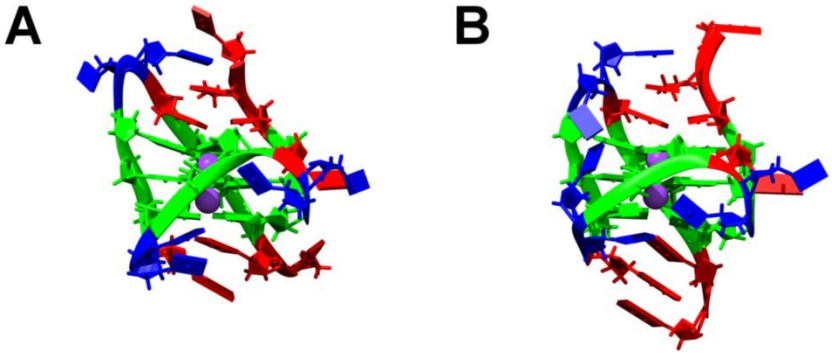

Figure S7. Cartoon depictions of representative structures from cluster analysis of the 2HY9 MD trajectory. The clusters are shown from the most populated cluster to the least populated cluster. Nucleotides are colored according to NDB formats: guanine is green, adenine is red, and thymine is blue. Potassium ions are colored purple.

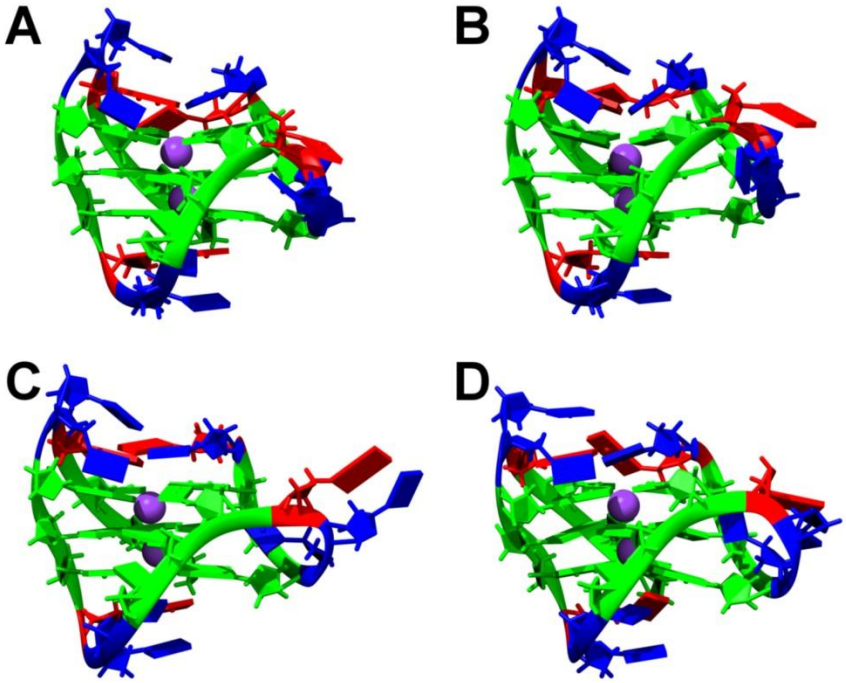

Figure S8. Cartoon depictions of representative structures from cluster analysis of the 2JSM MD trajectory. The clusters are shown from the most populated cluster to the least populated cluster. Nucleotides are colored according to NDB formats: guanine is green, adenine is red, and thymine is blue. Potassium ions are colored purple.

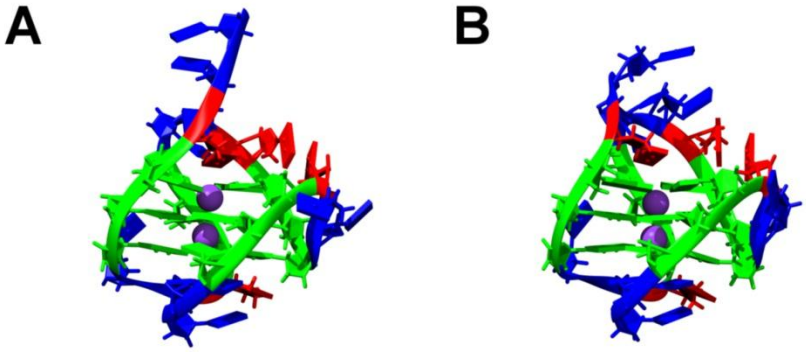

Figure S9. Cartoon depictions of representative structures from cluster analysis of the 2JPZ MD trajectory. The clusters are shown from the most populated cluster to the least populated cluster. Nucleotides are colored according to NDB formats: guanine is green, adenine is red, and thymine is blue. Potassium ions are colored purple.

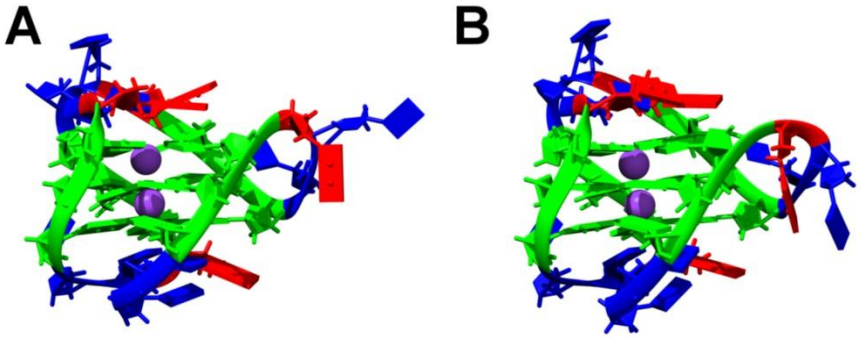

Figure S10. Cartoon depictions of representative structures from cluster analysis of the 2JSL MD trajectory. The clusters are shown from the most populated cluster to the least populated cluster. Nucleotides are colored according to NDB formats: guanine is green, adenine is red, and thymine is blue. Potassium ions are colored purple.

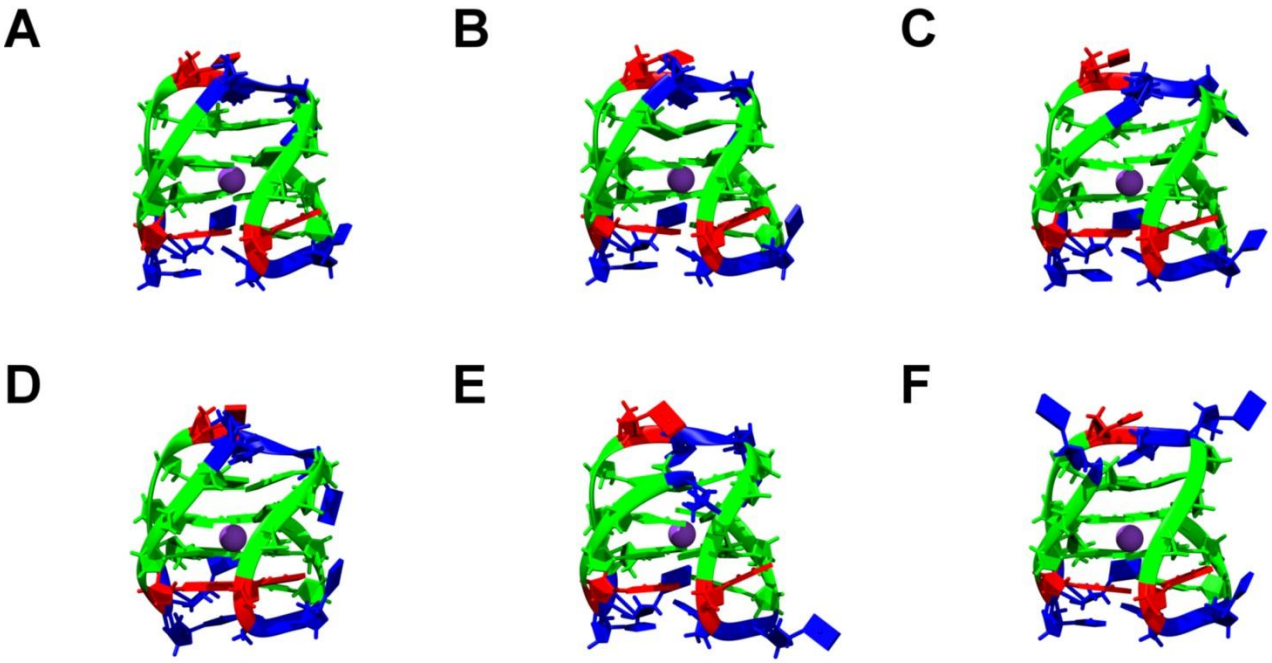

Figure S11. Cartoon depictions of representative structures from cluster analysis of the 2KF8 MD trajectory. The clusters are shown from the most populated cluster to the least populated cluster. Nucleotides are colored according to NDB formats: guanine is green, adenine is red, and thymine is blue. Potassium ions are colored purple.

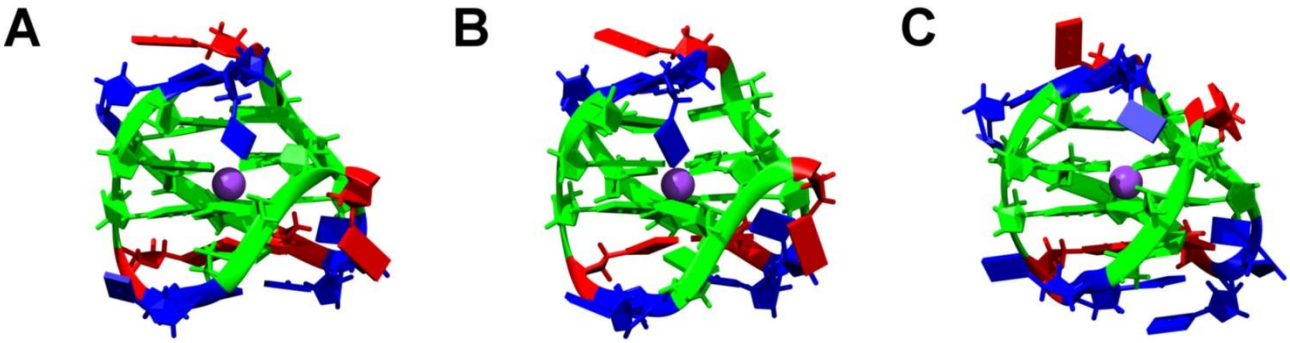

Figure S12. Cartoon depictions of representative structures from cluster analysis of the 2KKA-G MD trajectory. The clusters are shown from the most populated cluster to the least populated cluster. Nucleotides are colored according to NDB formats: guanine is green, adenine is red, and thymine is blue. Potassium ions are colored purple.

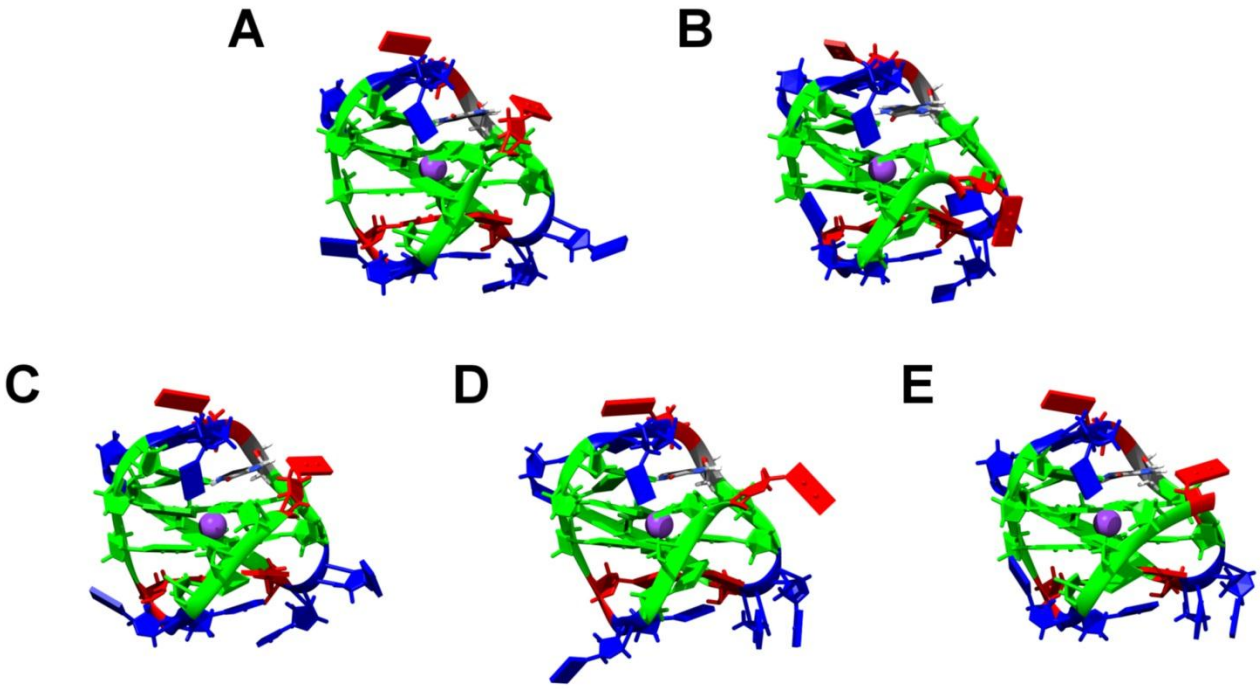

Figure S13. Cartoon depictions of representative structures from cluster analysis of the 2KKA-I MD trajectory. The clusters are shown from the most populated cluster to the least populated cluster. Nucleotides are colored according to NDB formats: guanine is green, adenine is red, and thymine is blue. Potassium ions are colored purple.

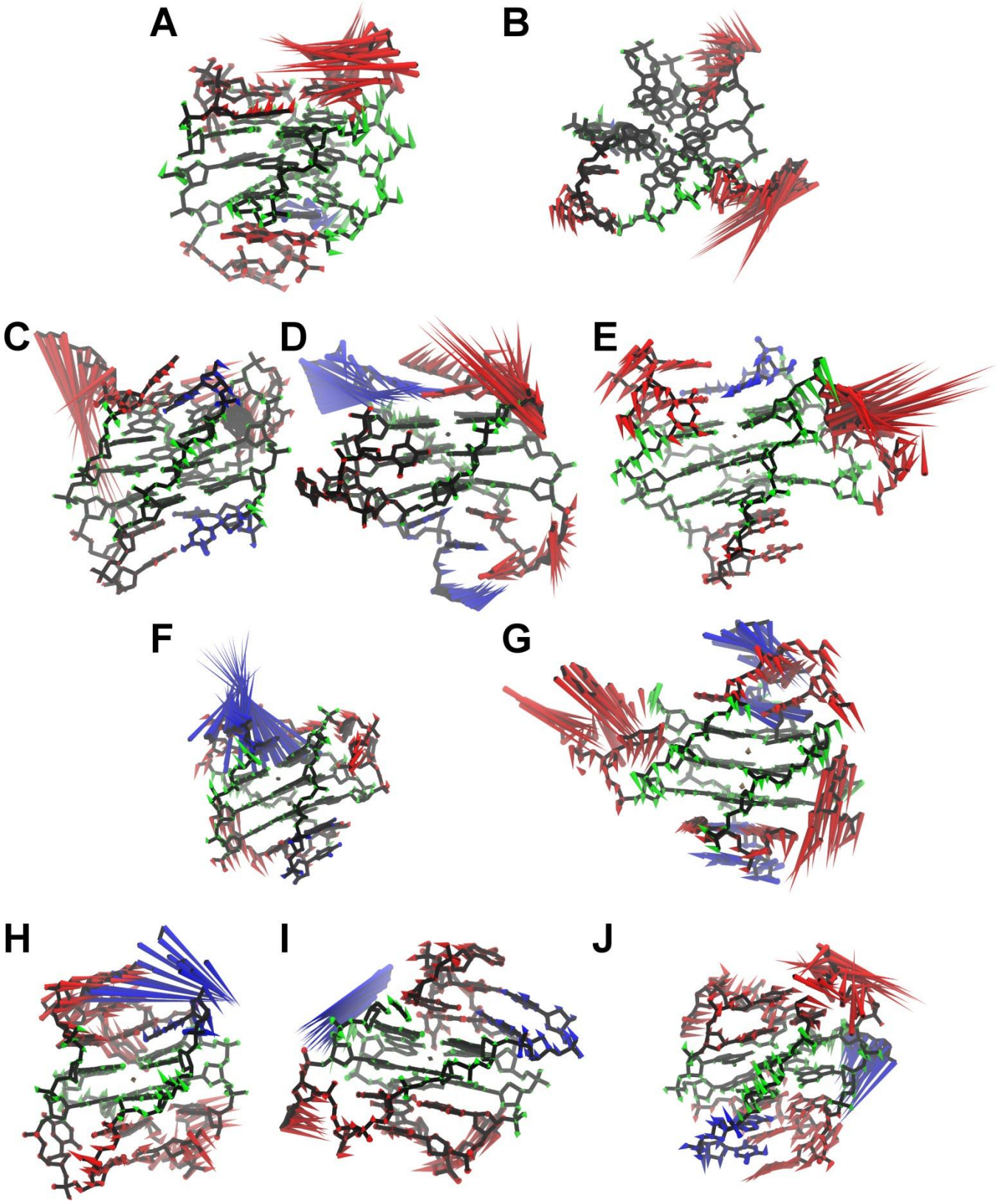

Figure S14. Porcupine plots of the second eigenvectors for 143D (A), 1KF1 (B), 2GKU (C), 2HY9 (D), 2JSM (E), 2JPZ (F), 2JSL (G), 2KF8 (H), 2KKA-G (I), and 2KKA-I(J). Motions associated with stem residues are colored green, loop residues are red, flanking residues are blue, and central ions are yellow.

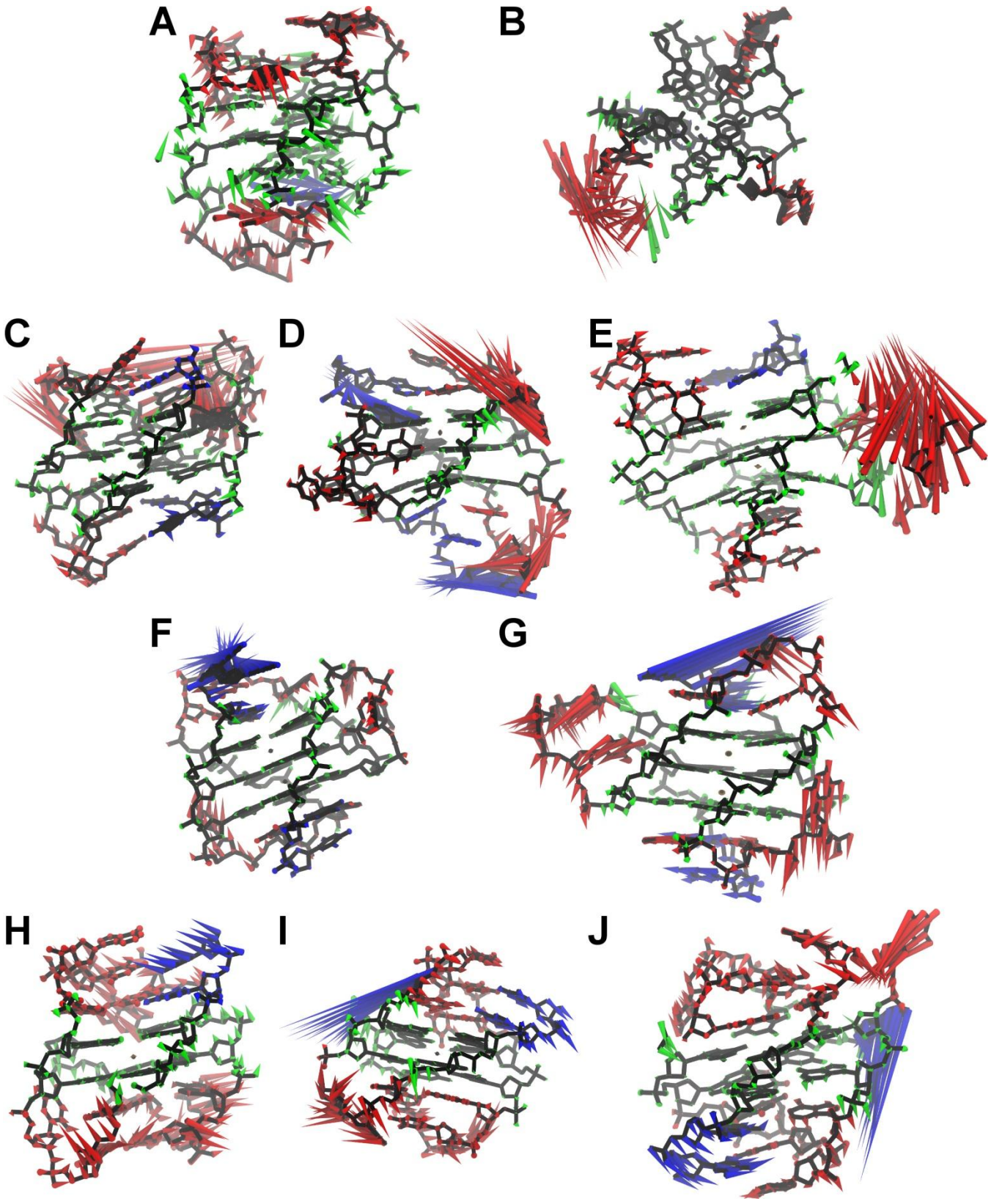

Figure S15. Porcupine plots of the third eigenvectors for 143D (A), 1KF1 (B), 2GKU (C), 2HY9 (D), 2JSM (E), 2JPZ (F), 2JSL (G), 2KF8 (H), 2KKA-G (I), and 2KKA-I(J). Motions associated with stem residues are colored green, loop residues are red, flanking residues are blue, and central ions are yellow.

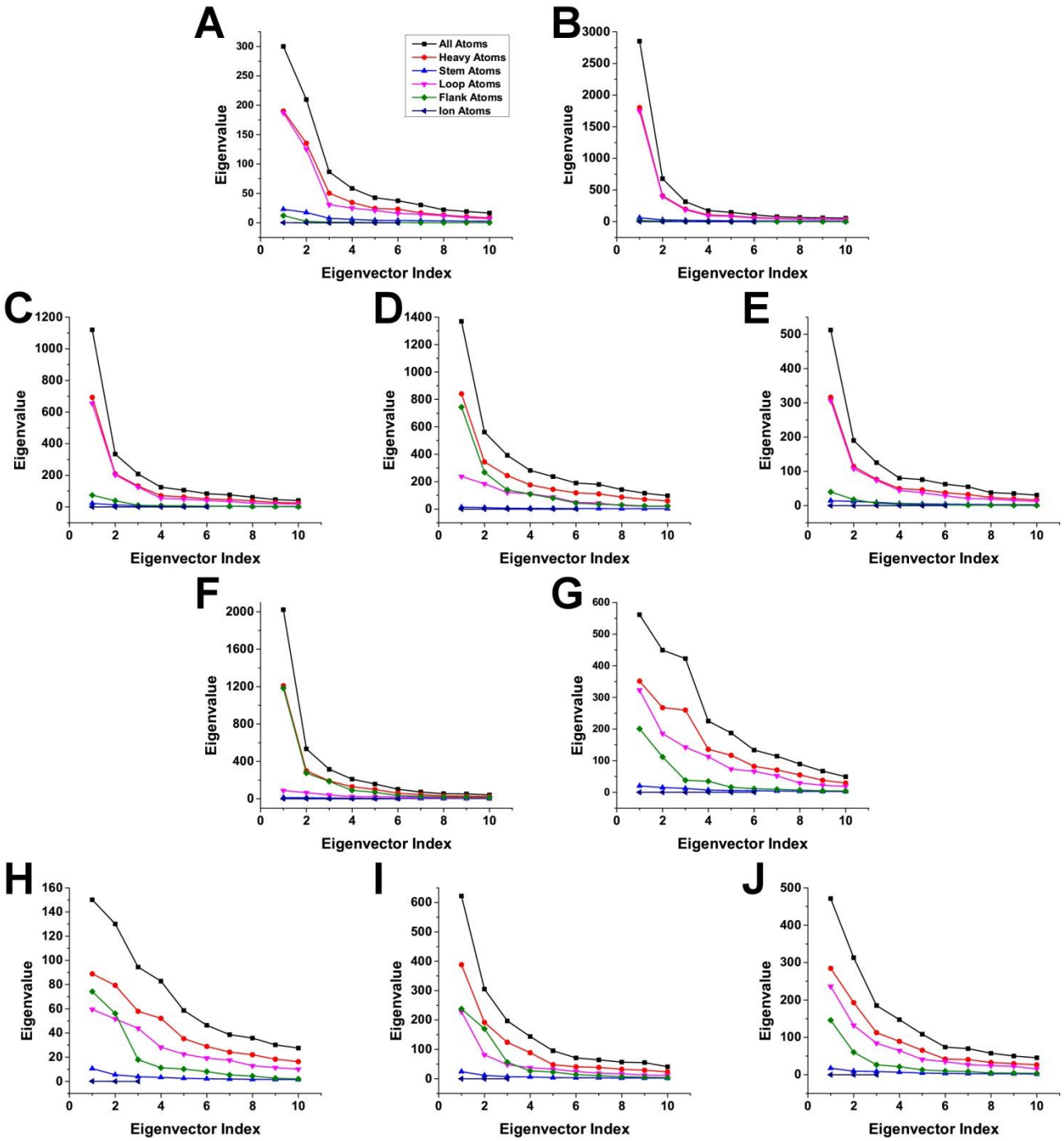

Figure S16. The first ten eigenvalues for 143D (A), 1KF1 (B), 2GKU (C), 2HY9 (D), 2JSM (E), 2JPZ (F), 2JSL (G), 2KF8 (H), 2KKA-G (I), and 2KKA-I(J).

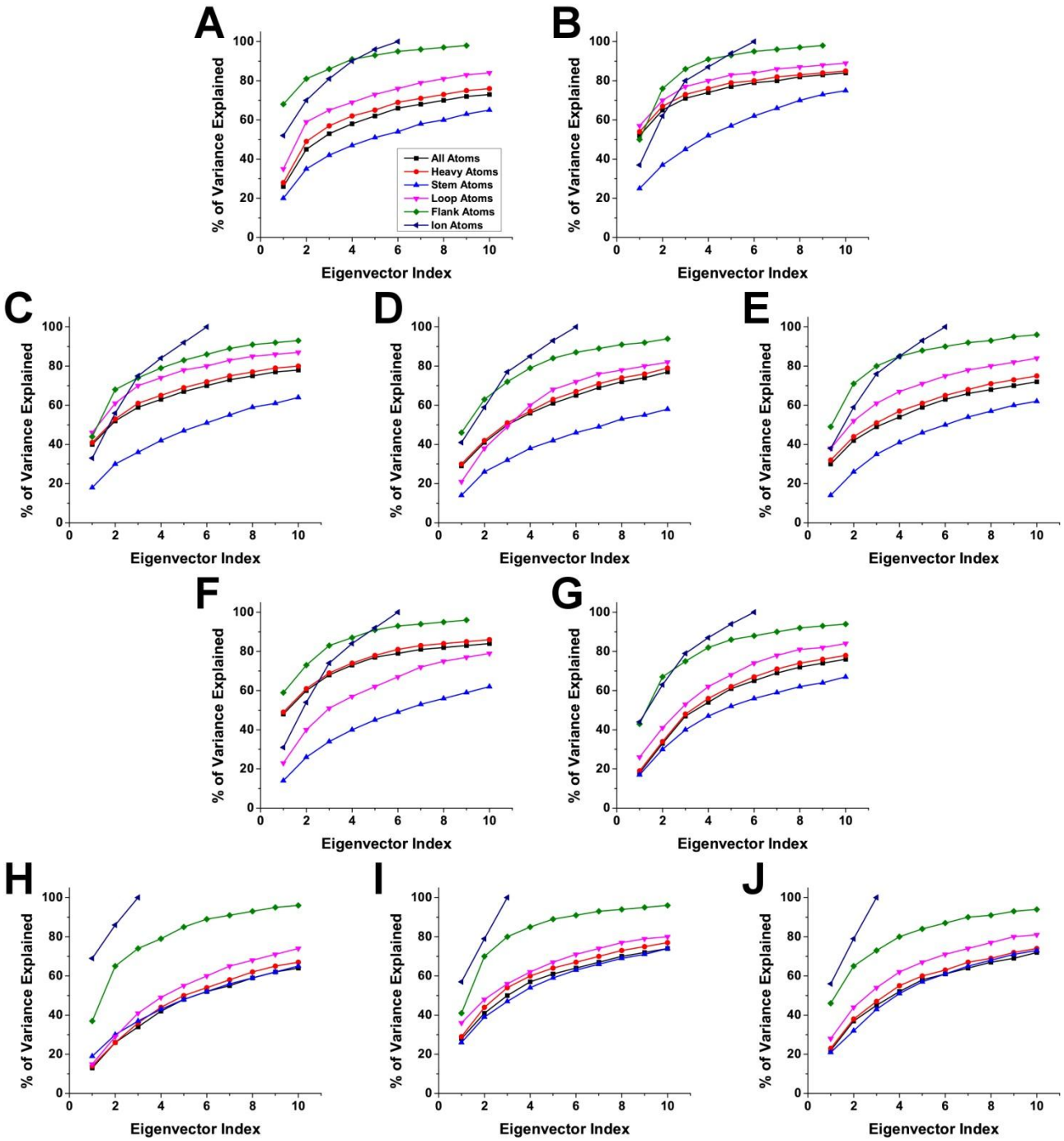

Figure S17. The percent of total variance explained by principal component analysis for 143D (A), 1KF1 (B), 2GKU (C), 2HY9 (D), 2JSM (E), 2JPZ (F), 2JSL (G), 2KF8 (H), 2KKA-G (I), and 2KKA-I(J).

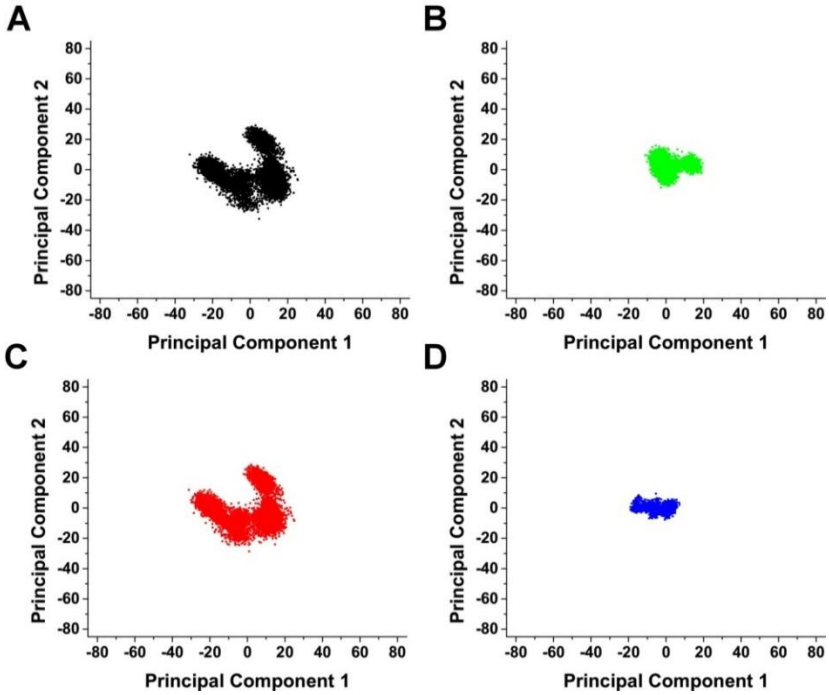

Figure S18. The second principal component as a function of the first principal component for 143D MD trajectory. Principal components are plotted for all non-hydrogen atoms (A), non-hydrogen G-tetrad stem atoms (B), non-hydrogen loop atoms (C), and non-hydrogen flanking bases atoms (D). For the 143D MD trajectory, dynamic motions of loop atoms have a dominant effect on the overall dynamic motions of the G-quadruplex structures.

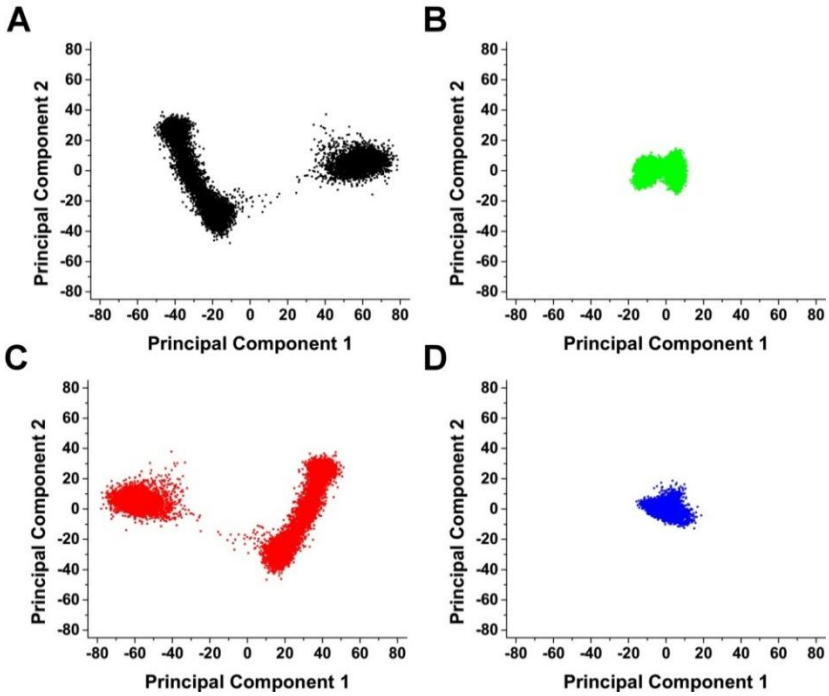

Figure S19. The second principal component as a function of the first principal component for 1KF1 MD trajectory. Principal components are plotted for all non-hydrogen atoms (A), non-hydrogen G-tetrad stem atoms (B), non-hydrogen loop atoms (C), and non-hydrogen flanking bases atoms (D). For the 1KF1 MD trajectory, dynamic motions of loop atoms have a dominant effect on the overall dynamic motions of the G-quadruplex structures.

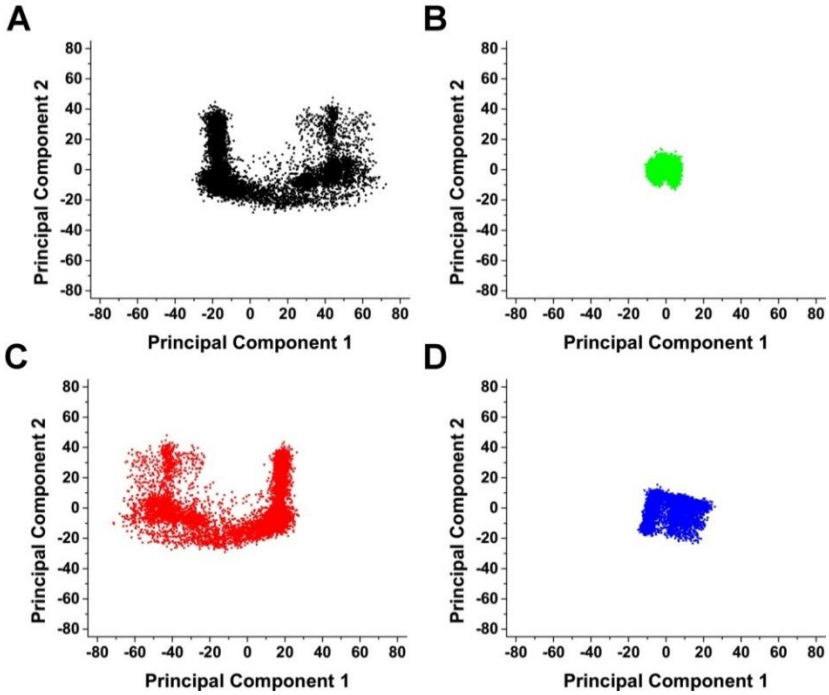

Figure S20. The second principal component as a function of the first principal component for 2GKU MD trajectory. Principal components are plotted for all non-hydrogen atoms (A), non-hydrogen G-tetrad stem atoms (B), non-hydrogen loop atoms (C), and non-hydrogen flanking bases atoms (D). For the 2GKU MD trajectory, dynamic motions of loop atoms have a dominant effect on the overall dynamic motions of the G-quadruplex structures.

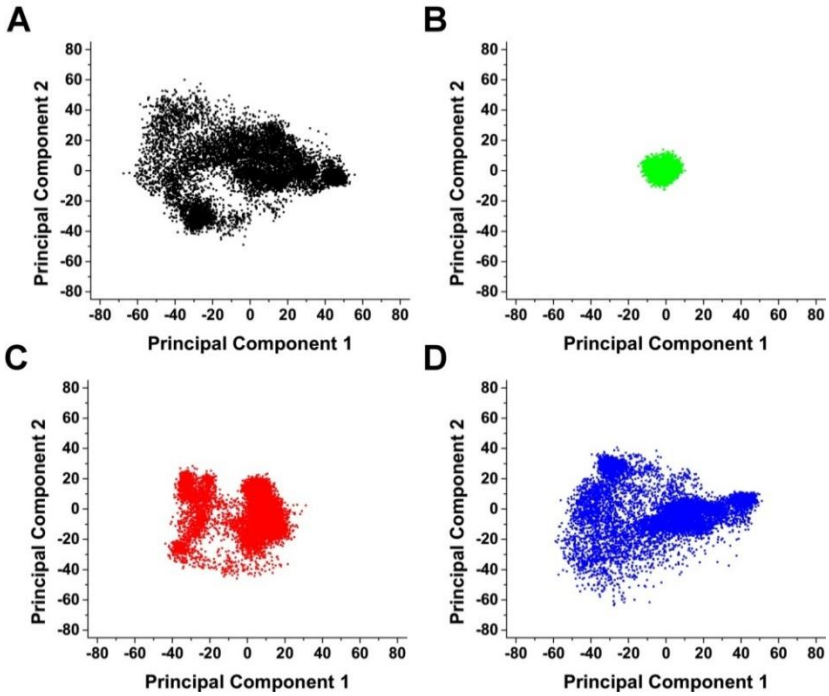

Figure S21. The second principal component as a function of the first principal component for 2HY9 MD trajectory. Principal components are plotted for all non-hydrogen atoms (A), non-hydrogen G-tetrad stem atoms (B), non-hydrogen loop atoms (C), and non-hydrogen flanking bases atoms (D). For the 2HY9 MD trajectory, dynamic motions of flanking atoms have a dominant effect on the overall dynamic motions of the G-quadruplex structures with only small contributions from loop atoms.

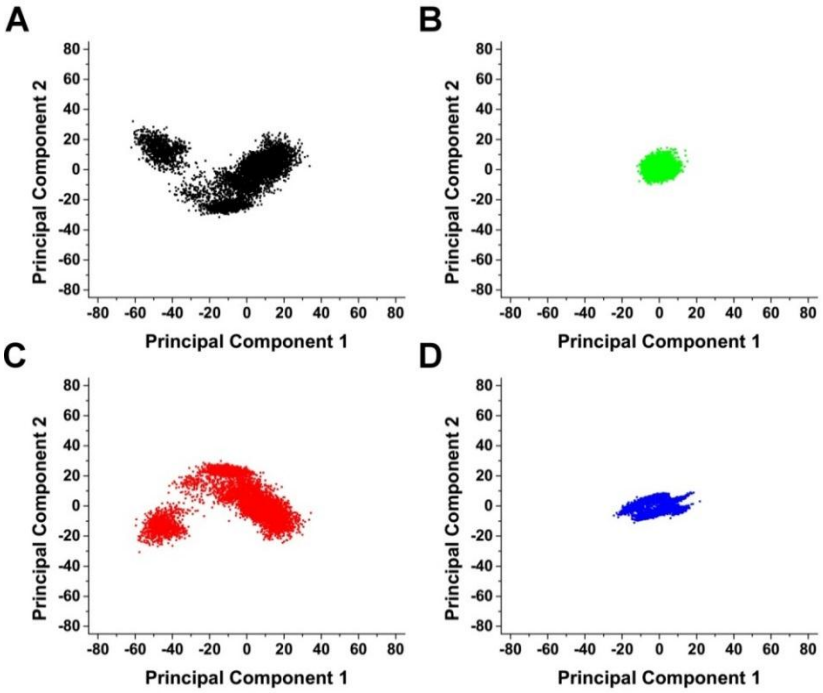

Figure S22. The second principal component as a function of the first principal component for 2JSM MD trajectory. Principal components are plotted for all non-hydrogen atoms (A), non-hydrogen G-tetrad stem atoms (B), non-hydrogen loop atoms (C), and non-hydrogen flanking bases atoms (D). For the 2JSM MD trajectory, dynamic motions of loop atoms have a dominant effect on the overall dynamic motions of the G-quadruplex structures.

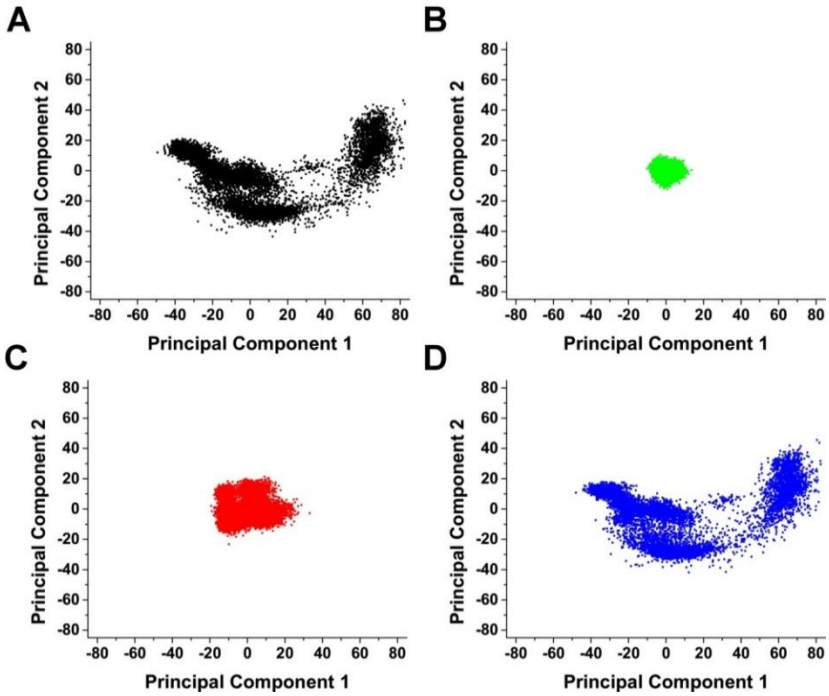

Figure S23. The second principal component as a function of the first principal component for 2JPZ MD trajectory. Principal components are plotted for all non-hydrogen atoms (A), non-hydrogen G-tetrad stem atoms (B), non-hydrogen loop atoms (C), and non-hydrogen flanking bases atoms (D). For the 2JPZ MD trajectory, dynamic motions of flanking atoms have a dominant effect on the overall dynamic motions of the G-quadruplex structures.

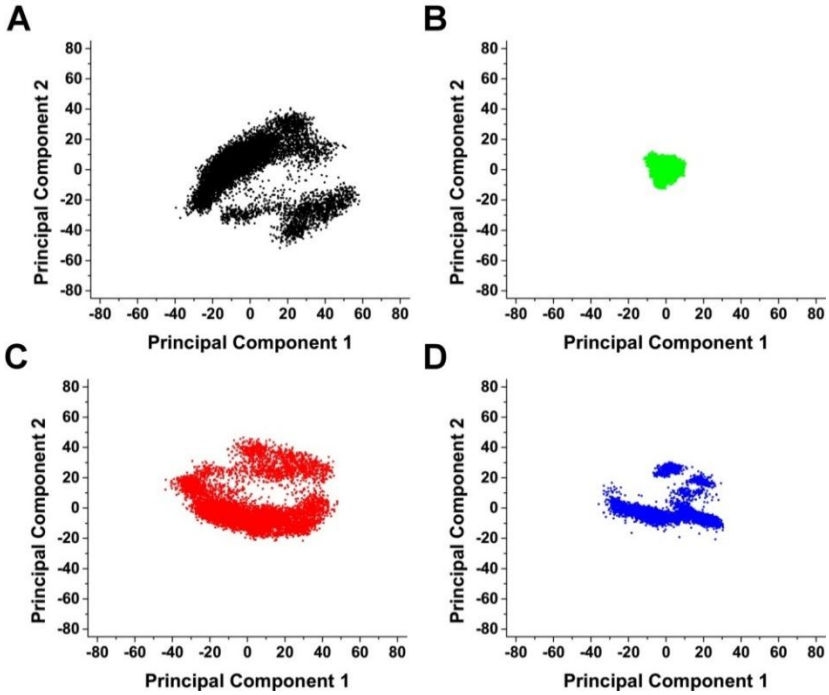

Figure S24. The second principal component as a function of the first principal component for 2JSL MD trajectory. Principal components are plotted for all non-hydrogen atoms (A), non-hydrogen G-tetrad stem atoms (B), non-hydrogen loop atoms (C), and non-hydrogen flanking bases atoms (D). For the 2JSL MD trajectory, dynamic motions of both loop and flanking atoms were observed to influence the overall dynamic motions of the G-quadruplex structures.

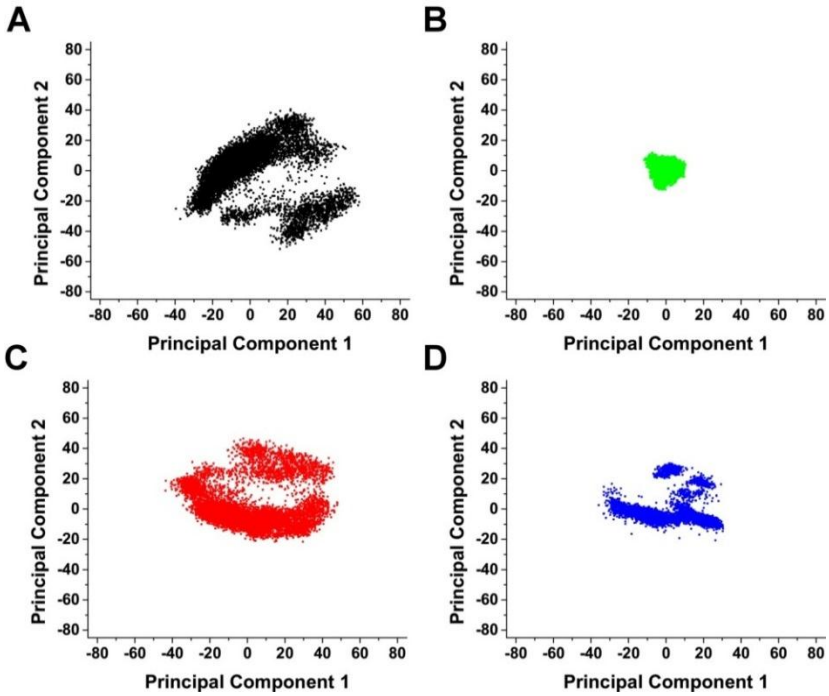

Figure S25. The second principal component as a function of the first principal component for 2KF8 MD trajectory. Principal components are plotted for all non-hydrogen atoms (A), non-hydrogen G-tetrad stem atoms (B), non-hydrogen loop atoms (C), and non-hydrogen flanking bases atoms (D). For the 2KF8 MD trajectory, dynamic motions of both loop and flanking atoms were observed to influence the overall dynamic motions of the G-quadruplex structures.

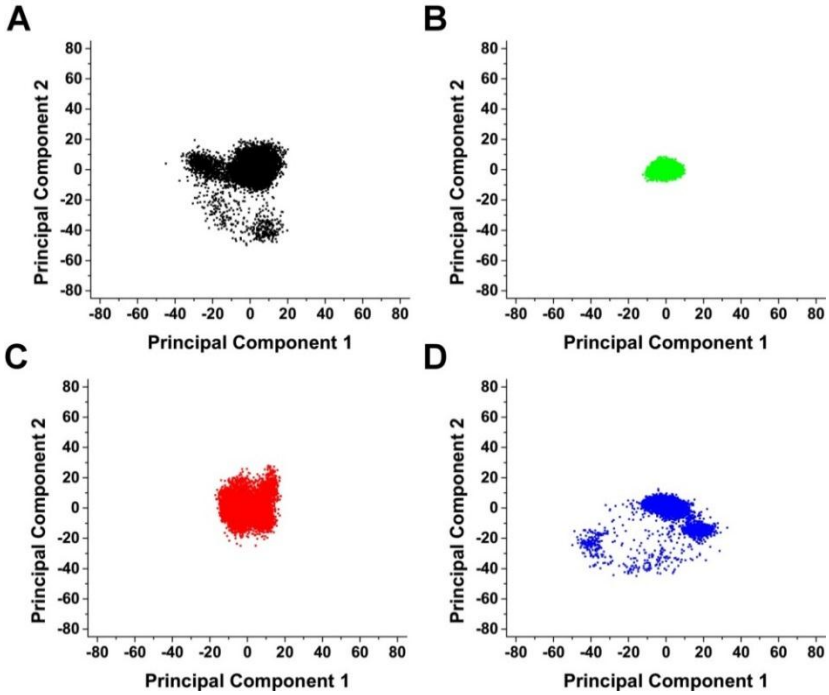

Figure S26. The second principal component as a function of the first principal component for 2KKA-G MD trajectory. Principal components are plotted for all non-hydrogen atoms (A), non-hydrogen G-tetrad stem atoms (B), non-hydrogen loop atoms (C), and non-hydrogen flanking bases atoms (D). For the 2KKA-G MD trajectory, dynamic motions of both loop and flanking atoms were observed to influence the overall dynamic motions of the G-quadruplex structures.

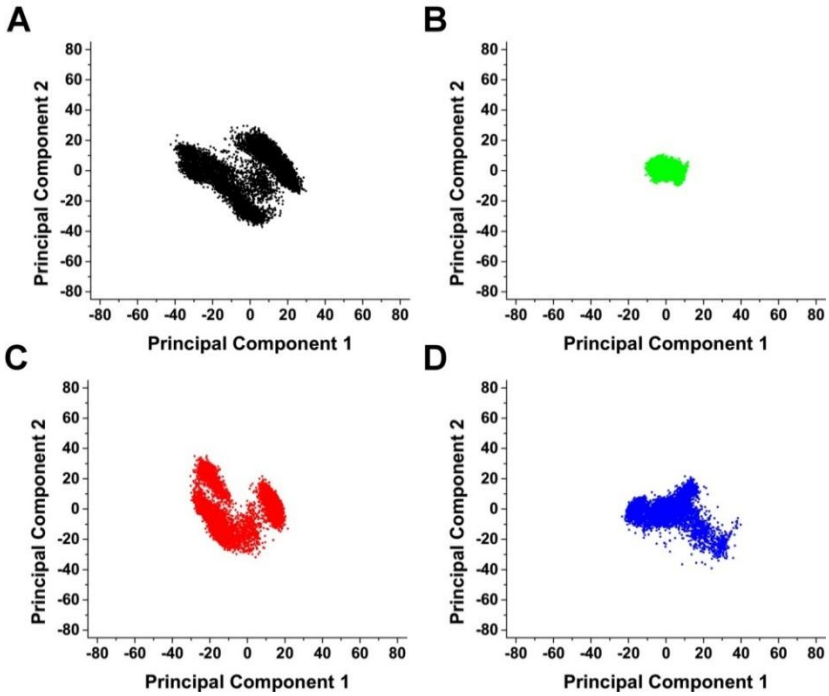

Figure S27. The second principal component as a function of the first principal component for 2KKA-I MD trajectory. Principal components are plotted for all non-hydrogen atoms (A), non-hydrogen G-tetrad stem atoms (B), non-hydrogen loop atoms (C), and non-hydrogen flanking bases atoms (D). For the 2KKA-I MD trajectory, dynamic motions of both loop and flanking atoms were observed to influence the overall dynamic motions of the G-quadruplex structures.

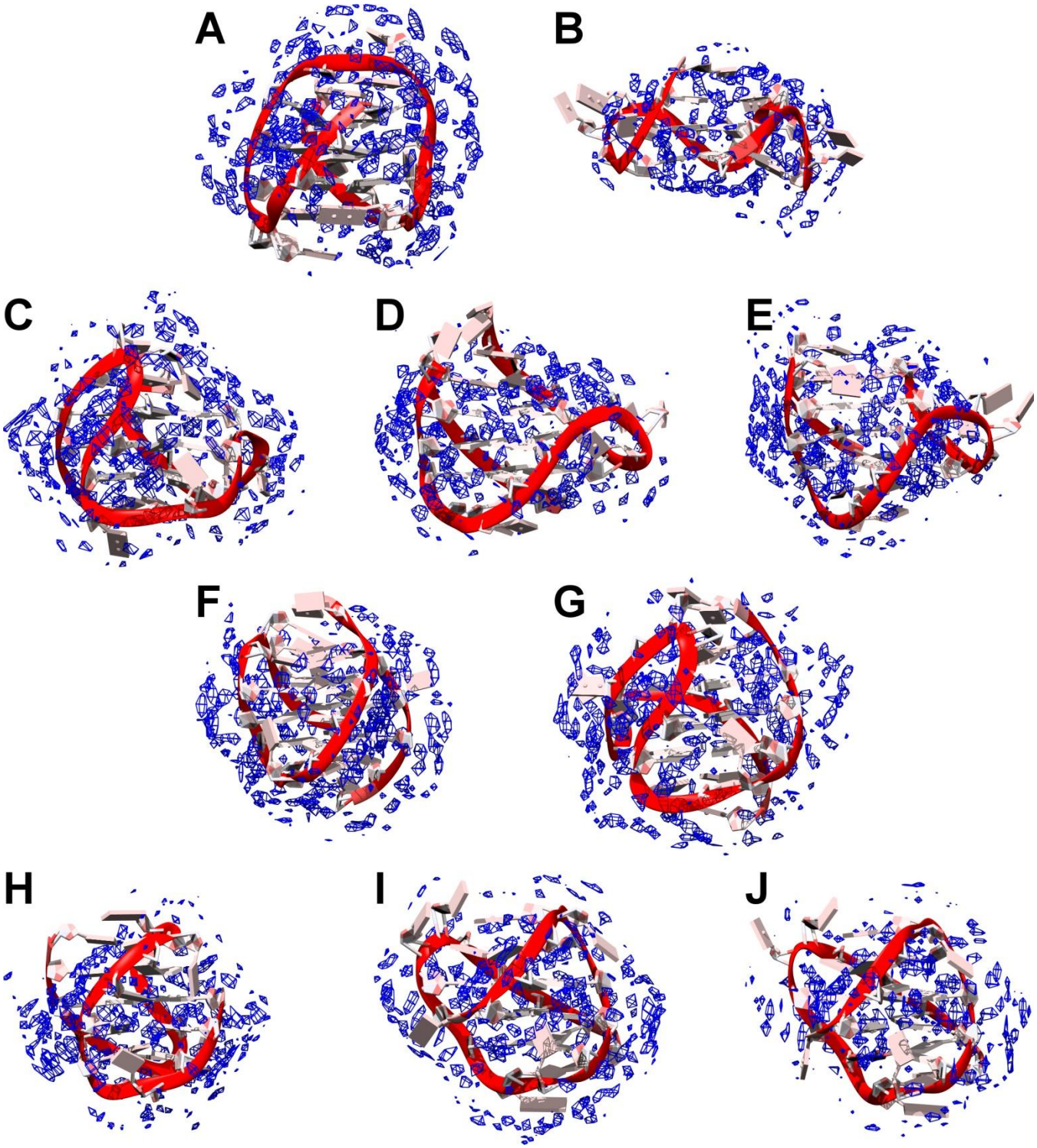

Figure S28. Pseudo-density grid maps of water oxygen atoms for 143D (A), 1KF1 (B), 2GKU (C), 2HY9 (D), 2JSM (E), 2JPZ (F), 2JSL (G), 2KF8 (H), 2KKA-G (I), and 2KKA-I (J). Water density (blue) was contoured at 2X the density (55.5 M) of bulk water. The average structure of each G-quadruplex over the trajectory is shown.

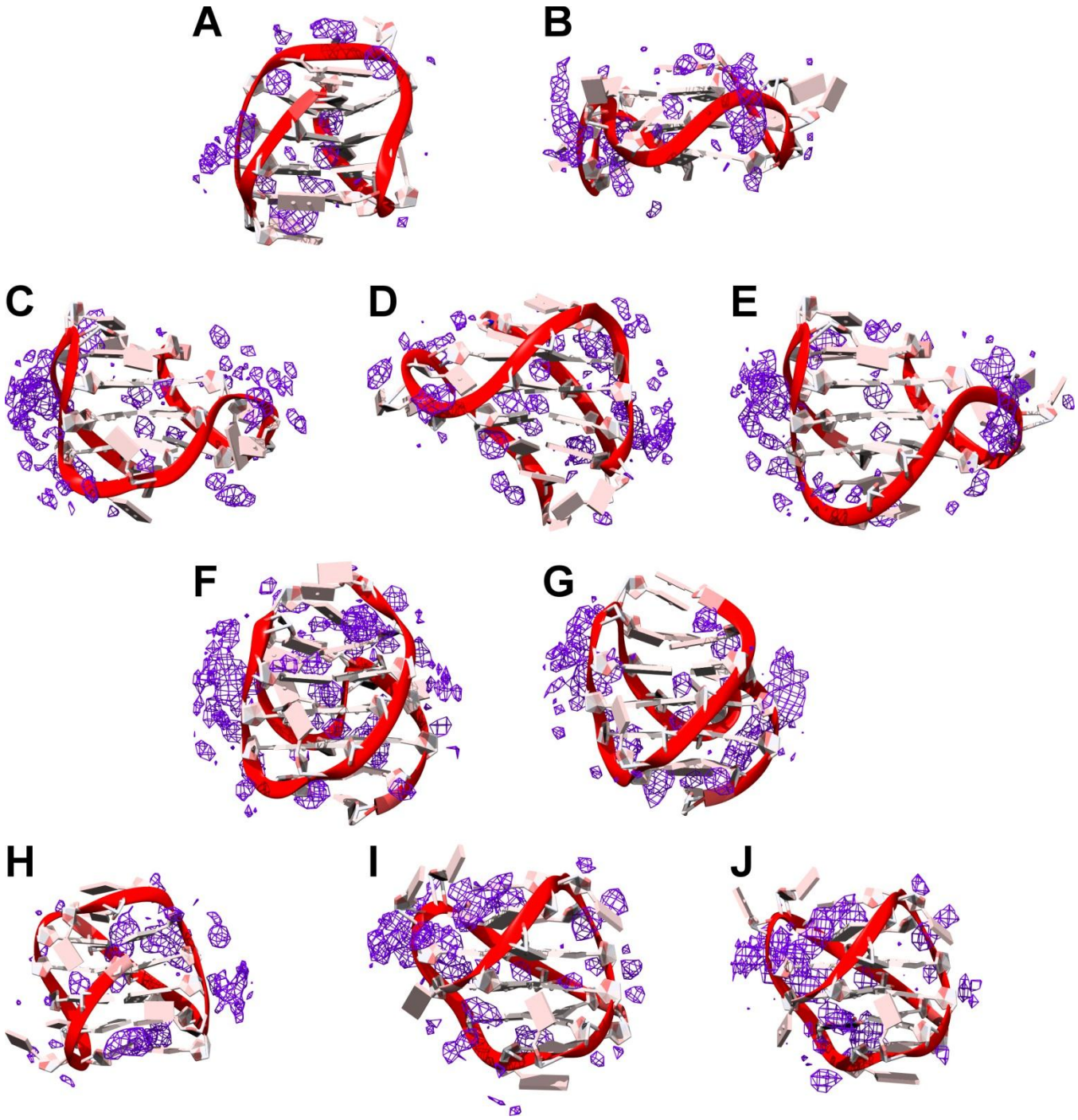

Figure S29. Pseudo-density grid maps of cations for 143D (A), 1KF1 (B), 2GKU (C), 2HY9 (D), 2JSM (E), 2JPZ (F), 2JSL (G), 2KF8 (H), 2KKA-G (I), and 2KKA-I (J). Cations density (purple) was contoured at the solubility density of sodium (6 M) for 143D and at the solubility density of potassium (4 M) for the other G-quadruplex structures. The average structure of each G-quadruplex over the trajectory is shown.